Proceedings of the ASME 2013 International Technical Conference and Exhibition on Packaging and Integration of Electronic and Photonic Microsystems
InterPACK2013
July 16-18, 2013, Burlingame, CA, USA

IPACK2013-73104

A METHOD FOR FAILURE ANALYSIS FOR DEVICES WITH SIMULTANEOUS IMAGING OF ELECTRON EMISSION AND NEAR IR THERMOREFLECTANCE

Kazuaki Yazawa
Microsanj LLC and Purdue University
West Lafayette, IN, USA

Dustin Kendig
Microsanj LLC.
Santa Clara, CA, USA

James Christofferson
Microsanj LLC.
Santa Clara, CA, USA

Ali Shakouri
Purdue University
West Lafayette, IN, USA

ABSTRACT

Thermal characterization is useful for identifying the cause of circuit failures. Unusually high local temperatures can occur due to unexpected and localized power dissipation in a particular device, which was not anticipated nor designed in the device. Unintended high temperatures may be the source of circuit damage or it might be caused by the failure itself, such as a tiny short-circuit. However, it is often difficult to obtain enough information about the physical structure and characteristics of the circuit to clearly identify the cause of the failure. The method we present here is an imaging technique with both thermal distribution and emission intensity superimposed on a single image.

Thermoreflectance thermal imaging takes advantage of the differences in light reflectivity of the surface with a changing temperature. This relationship is quite linear in a typical temperature range of interest. Using 1300 nm wave length for the illuminating source, the metal circuitry of interest is directly observed through the almost transparent silicon substrate of a flip chip mounted device. With the same photo detecting imaging sensor, i.e. InGaAs junction array, the emission from the target device through the silicon substrate is also detected. If there are some local electron collisions, e.g. due to a current concentration at a defect or a tiny whisker, a localized excess energy by electron-electron collision yields the photon generation and emits an electromagnetic wave. The photons having a sufficient energy level at wavelength transparent to silicon, reach the photo detecting imaging sensor. With software processing and precise synchronization of the driving circuit, illumination, and imaging, we can separate the thermal signal from the emission and observe transient behavior on a nanosecond time scale. The time response is helpful in some cases to separate cause and effect. As an example, an unintended small short-circuit resulting from the fabrication process may be reproduced for a small number of samples. The emission would be observed first, followed by the thermal signal which propagates in time. Another example is for a circuit with low design margin, in this case only a single sample exhibits a difference between emission and/or thermal image while numbers of good samples are identical with respect to the emission and thermal image. This difference clearly indicates the location of a potential failure.

INTRODUCTION

Circuit integration and complexity is still exponentially increasing in logic ICs, thus creating more significant challenges with respect to the power density of hot spots [1]. One direction of higher integration, “More than Moore” [2], suggests an emerging growth of chip-stack packaging for a higher density packaging system required for: smart phones, pad type portable information systems, etc. There is also, growing demand for higher power density power devices [3, 4] and even photo-electric devices [5]. We developed and

Copyright © 2013 by ASME

utilized the thermoreflectance method [6] for thermal imaging and thermal characterization of the device under operating conditions.

As with thermal management issues, the defects and minor and local failures are getting more difficult to locate since the length scale of the device [7] and circuitry including wire traces, vias, and joints are getting smaller and smaller in highly complex geometrical arrangements. On the other hand, the reliability of these complex chips or chip packages cannot be relaxed. As is well known (see Ref. 8), the system reliability takes into account the root sum square of each failure rate as,

$$r = \sqrt{r_1^{\,2} + r_2^{\,2} + r_3^{\,2} + .. + r_n^{\,2}} \quad (1)$$

where, r_i is the individual failure rate and i is the index of the independent phenomena. Thus the failure analysis in the development phase and in-situ detection in the production phase is necessary and becomes more critical for recent devices and packages. Due to such variations, , non-contact and non-invasive methods are essential, especially for in-situ inspection. As one of the approaches, we studied the utilization of the preciously developed thermoreflectance technique to detect defects or to locate potential failures.

Thermoreflectance is an optical technique for obtaining the thermal response of a device without physically contacting the device. Time dependent thermoreflectance provides high spatial resolution 2D images in a time series comparable to the length scale of the device. In earlier work, we successfully took thermal images that indicated potential defects connecting to open circuits of 500 nm diameter copper via chains in a silicon substrate [9]. In that case a potential void creation caused by copper diffusion in the microstructure of the via was anticipated. We also used the same method to locate the defective spots in solar cells [10]. A new system development enables us to get images of the thermal signal through a silicon substrate and, simultaneously, obtain the photon emission from hot-electrons at the location of a concentrated current. A near-infrared (NIR) wavelength illuminating light source and InGaAs image sensor is integrated for this purpose. These components are commercially available so the system still consists of commodity components. The inter-locking technique and software image processing [11] provide this state-of-the-art new feature. In this paper, we will provide details of this method and its capability. We then show examples of this imaging technique.

NIR THERMOREFLECTANCE AND EMISSION

Thermoreflectance imaging, in general, is based on the physical relationship between the change in material reflectivity and the change in material temperature. A linear approximation of this relationship [12] is used when the temperature variation is small, such as the operation temperature of a CMOS chip relative to room temperature, e.g. 20 ^{o}C to 120 ^{o}C. The relationship is described, using the thermoreflectance coefficient C_{th} as,

$$\frac{\Delta R}{R} = \left(\frac{1}{R} \frac{\partial R}{\partial T} \right) \Delta T = C_{th} \Delta T \quad (2)$$

where, R is the intensity of reflectance for the surface material averaged over the target area. The thermoreflectance spectrum for semiconductor materials was described in 1968 [13]. A more specific technique for the novel imaging setup was suggested in Ref. 14. This imaging technique uses a probing light source to measure the change in reflected light. The probing light is pulsed to measure the temperature at specified time delays with respect to the biasing pulse applied to heaters on the chip, or with respect to the operating pulse of the chip. In some cases, we operate the chip to have a logic circuit initialized and then apply a modified bias to the circuit with an external power source. The magnitude of the reflectivity change with temperature is called the thermoreflectance coefficient. The thermoreflectance coefficient is non-zero for most wavelengths in the visible range. We have adapted a differencing lock-in technique to obtain a full field, mega-pixel thermal transient of the devices with mature CCD imaging technology. This is different from the ordinary lock-in technique that uses an excitation with a 50% duty cycle and sine wave approximations of the thermal signal. The setup described can generally achieve a time resolution of 100 ns. Results in university research with a pulsed laser [15] have shown that 800 ps is achievable. The transient system works by opening the camera shutter and pulsing the light source. The pulsed light source samples the change in temperature of the device at a given delay with respect to the start of the excitation pulse. This thermal transient information is particularly useful as it can show the heat diffusion from microscale hot spots or features on the chip down to the thermal interface material and the package [16].

The NIR light, with wavelengths ranging from 900 nm to 1300 nm, can be used in the same way as visible light. Insofar as the surface is opaque to a particular wavelength, we can detect the reflection and thus detect a reflection intensity change with changing temperature. If the substrate is transparent, e.g. pure silicon is nearly transparent at 1300 nm wavelength at room temperature [17]; we can observe the reflection of the wire trace or opaque oxide materials underneath the silicon substrate by ‘seeing through’ the substrate. As is well known, the incoherent light wave

Copyright © 2013 by ASME

diffracts, thus the limitation of spatial resolution is in the order of d,

$$d = \frac{\lambda}{2(n\sin\theta)} \tag{3}$$

where, λ is the wavelength of the illuminating light source, $n\sin\theta$ is the numerical aperture, θ is a half angle from the light source over the entire optical system, and n is the index of refraction. Based on the optics of the microscope, $n\sin\theta$ is approximately equal to 1 and $d \approx \lambda/2$ for a typical microscope. This value depends on the optics and is not affected by the target surface. The resolution of the thermal images is exactly the same as the resolution of the microscopy since we measure the optical response. The wavelength and the optics of the microscope, therefore, limit the spatial resolution of the thermal images. Local heating less than the spatial resolution limit can still provide a number of blurred pixels due to thermal diffusion. These images will be clearer if a transient measurement is made [6].

The NIR wavelength is carefully chosen to maintain the spatial resolution in the range of a micron for imaging through a silicon substrate.

In this electro-magnetic wavelength range, we also observe photons emitted from 1) electron-hole recombination as well as 2) generated hot-electrons colliding with the lattice with much larger probability compared to the normal electron-phonon energy exchange. The electrons are given excess energy over the band-gap of atoms and generate photons.
Based on Planck's law, the temperature dependent radiation spectrum I(T) from a black body is found as a function of wavelength, λ, as,

$$I(T) = \frac{2hc^2}{\lambda^5}\frac{1}{e^{\frac{hc}{\lambda k_B T}} - 1} \tag{4}$$

where, h is Planck's constant, c is the speed of light, k_B is Boltzmann's constant, and T is the absolute temperature of the surface. The peak wavelength, $\lambda_{max,}$ is found by Wien's displacement law as,

$$\lambda_{max} = \frac{b}{T} \tag{5}$$

where, b=2.898 x10^{-3} [K.m].

Emission Microscopy (EMMI) has been commonly used for failure detection with a combination of cryogenically cooled InGaAs photon detectors. The reason for cooling the imaging device is to reduce the dark current. This is completely replaceable by a camera with a cryogenic cooler if the intensity resolution of emission alone is more important than the investment. In any case, the temperature resolution for thermoreflectance is not affected.

The local emission in NIR wavelength suggests a potential defect. Various NIR studies are summarized in [18]. The sources of the emission by colliding electrons are potentially the conflict of current flow caused by an unwanted short circuit, or a large contraction of current flow, etc. Most of the devices or local circuits are not usually designed to handle such extremely high current densities. Therefore, the strength of emission suggests the level of the defects or can be an indication of damage. At some point in the future, these causes of emission may degrade the performance or functionality of the circuits. This is primarily due to the rate of increasing local temperature following the modified Arrhenius law, Eq. (6), which suggests that the chemical reaction due to the defect is exponentially accelerated by temperature, T, and with n^{th} power of the ratio to the reference temperature, T_{ref}. The rate constant, k, is found as,

$$k = A(T/T_{ref})^n e^{-Ea/(RT)} \tag{6}$$

where, E_a is the activation energy of the reaction causing the defect or caused by the defect. The light generated by a defect is typically very faint. Therefore to detect the failure, the imaging device must have a very high photon sensitivity in the wavelength of interest (typically 1.0 to 1.8 microns using InGaAs or deep-depleted Silicon CCDs)

Photos of the system are shown in the Figs. 1a) and 1b) and the schematic is shown in Fig. 2.

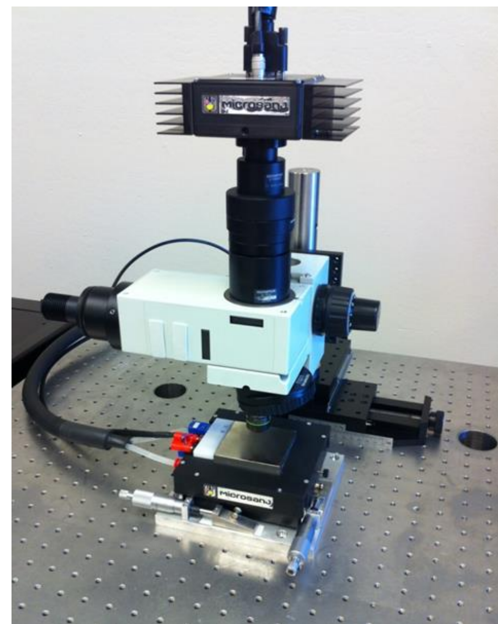

a)

Copyright © 2013 by ASME

b)

Figure 1: Picture of the system a) microscope setup and b) signal inter-lock and processing unit

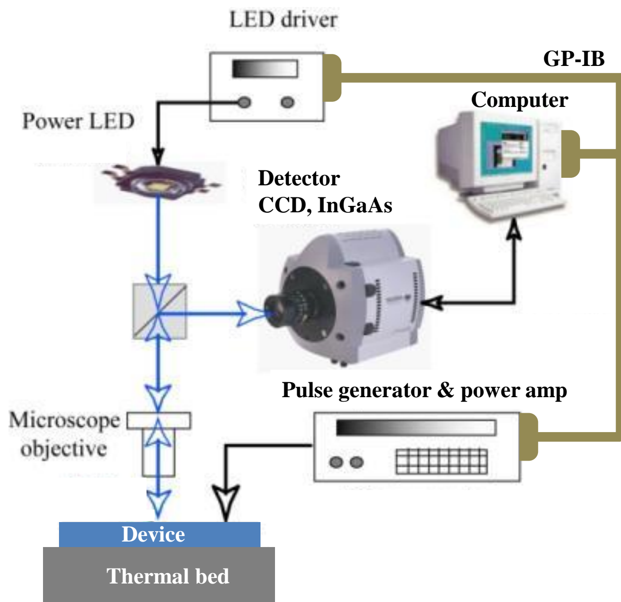

Figure 2: Schematic of the setup

RESULTS AND DISCUSSIONS

Two examples are presented in this paper. The first shows the unexpected heating found in the location where the powering up was not intended. 5x zoomed images show the location of the failure and the 20x zoomed image provides higher resolution (580 nm per pixel). Another example presents the simultaneous imaging of thermal and emission from the same location on the device with the same operating conditions with a 5x lens. With the 5x lens,, the spatial resolution is reduced to 2.4 µm per pixel.

Example 1: Wire-bonded chip

Fig. 3 shows the thermal intensity map of a wire-bonded chip mounted to a PCB board. The size of this Si-based chip is 1.6 mm x 1.1 mm with 500 µm thickness. The objective lens of the microscope is 20x corresponding to a field of view of 0.6 mm x 0.6 mm with a pixel resolution of 580 nm. We operated this device through the 8 gold wire-bonded connections to the pads. The circuit is initialized, and then we apply a pulse signal to V_{dd} of 0 V – 5.4 V to operate the active portion of interest under temporary extreme conditions. Under these conditions the current is latched until the supply is cycled off and on again. We used a 470 nm wavelength LED for this experiment and detected the reflectance with a CCD camera. Fig. 4 shows the time series of the thermal intensity contour maps of the device with a 5x lens with a corresponding field of view of 2.5 mm x 2.5 mm and a spatial resolution of 2.4 µm per pixel. As seen in the figure, the time response is shown to have different signal phases relative to the circuit delay. By analyzing the time delay, the operation of the circuit can be verified to be within the range of design tolerance, or out of the range. In this example, the time delay of interest for heating was 0.9-1.0 msec. This case illustrates the benefit of time dependent thermal characterization for understanding the circuit and its potential defects.

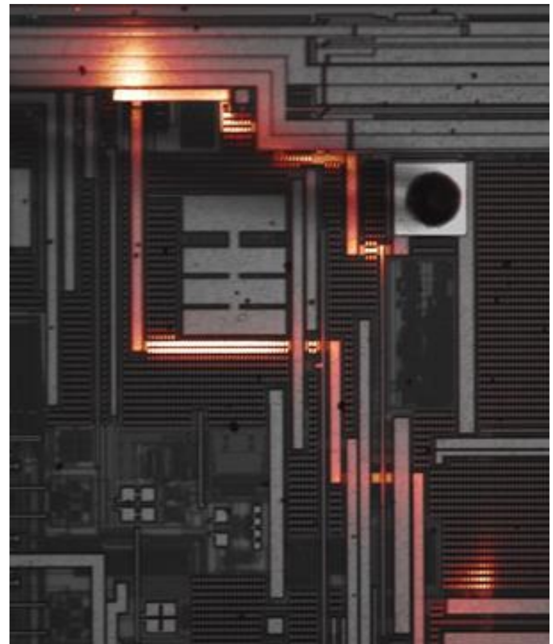

Figure 3: Device feature and thermal intensity map overlay with 20x objective

Copyright © 2013 by ASME

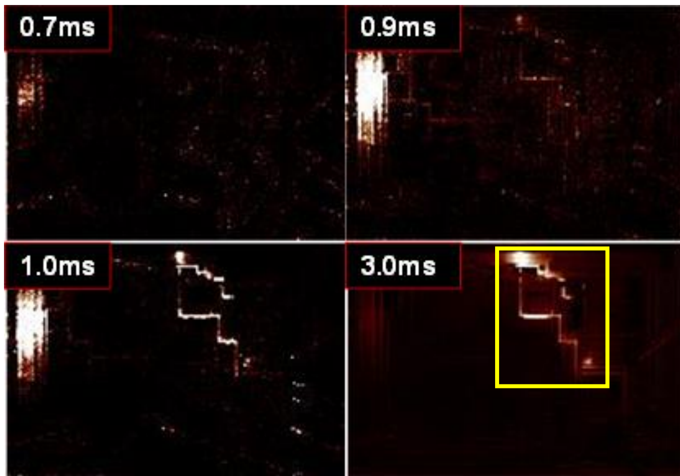

Figure 4: Thermal images in time series with 5x objective. The marked area in Fig. 4 heats up about 1 msec after the circuit begins to operate.

Fig. 5 also shows the temperature map on a color 3D plot. The thermoreflectance coefficient given by the linear relation between the reflection intensity and the temperature for this device surface was 1.0e-4. This is an approximate value for this complex materials surface based on our past experiences. The general method for determining the thermoreflectance coefficient is found in Ref. 14.

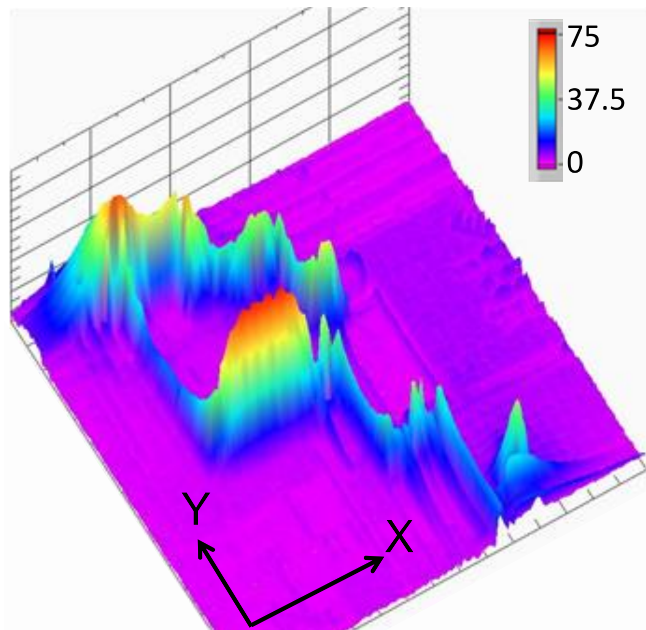

Figure 5: 3-D temperature contour plot for the same location as shown in Fig. 3 at a delay of 1.2 msec. Height along Z-axis with the color scale shows the temperature increase.

Example 2: Flip chip

Fig. 6 shows the emission intensity overlaid on the optical image of the device and Fig. 7 shows the thermoreflectance overlay for the same example. These are 5x zoom images of the 6.2 mm x 6.2 mm device with a flip-chip mount. The thickness of the silicon substrate is 450 µm, which is sufficiently thin to see through to the device layer from the backside. The wavelength of the LED illumination is 1300 nm while the InGaAs imaging sensor is sensitive between 0.9 and 1.7 µm in this setup. The pixels of the imaging sensor is 640 x 512. A group of three spots with 44 µW of emission power is observed at the indicated area in Fig. 6. The three spots are supposed to be the potential defects of transistors. The emission signal is sometimes very weak but the indication of electron collisions is clearly detected. The thermal map shows completely different hot spot locations, which are generating excessive heat from the high power density in the circuit. Two hotspots, indicated in Fig. 7, are the location of the arrays of vias connected to the back bumps to supply power to the circuitry of this chip.

Fig. 8 shows the time response of the temperature change at one of the locations marked in Fig. 7. The time constant of this temperature rise is approximately 10 msec, which ties to the feature of the circuit at the hot spot.

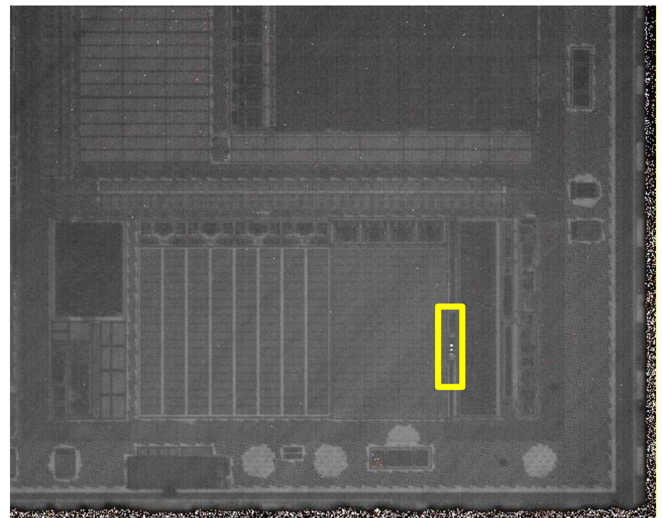

Figure 6: Emission intensity map over the optical image. Three spots are observed in the marked region with a 5x lens.

Copyright © 2013 by ASME

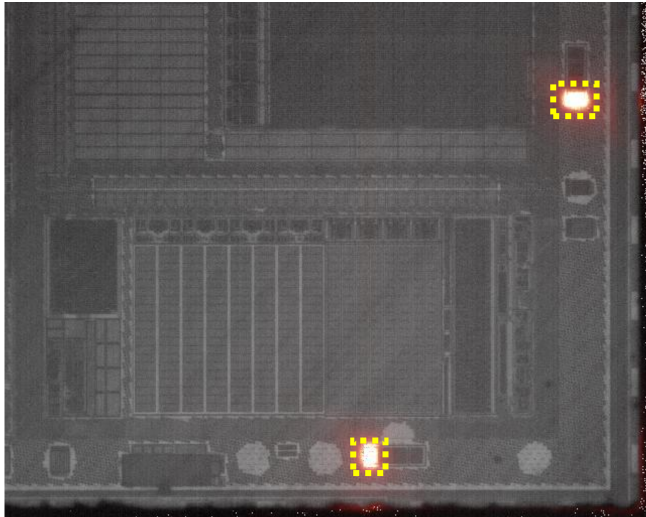

Figure 7: Thermoreflectance intensity map over the optical image with a 5x lens. This is the identical view of the device as in Fig 6under the same operating conditions. There are two hot spots marked in the picture, which are clearly observed in the thermal map but not seen in the emission map.

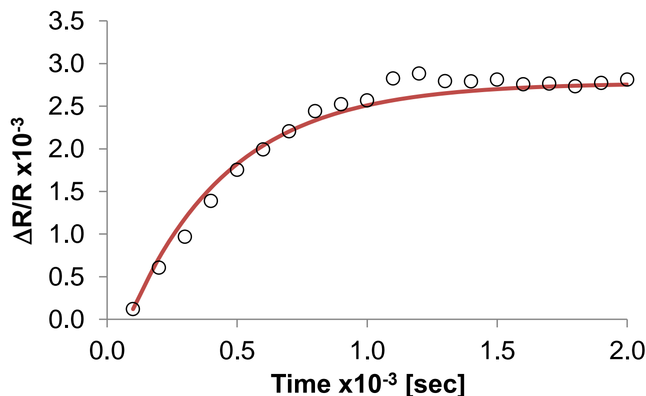

Figure 8: Reflectance change (relative temperature change) in time series for the top right highlighted region of Fig. 7.

In Fig. 8, the dots show the measured data and the curve shows the regression based on a single time constant, which is approximately 0.39 msec with 0.08 msec of a time delay.

CONCLUSIONS

We introduced the combined time-dependent NIR thermoreflectance and emission imaging method to uniquely detect and locate both temperature and emission hot spots. Both reflected light at the circuit layer, viewing through the silicon substrate, and the emitted photons from the same device with the same setup are mapped and overlaid. This particular sample showed completely independent locations for the emission hot spot and the thermal hot spot. Another example illustrated the detection of unwanted heating in transient mode for the operation of a circuit to help identify the location of a failure.

With transient imaging of emission and thermoreflectance, the cause and effect of the thermal irregularity will be capturedif both are connected.. This method is available with a micron scale spatial resolution, which is diffraction-limited by the optics, the wavelength of the illuminating light source, and the pixels of the detectors.

REFERENCES

[1] International Technology Roadmap for Semiconductors, ITRS 2011 Edition, http://www.itrs.net/Links/2011ITRS/Home2011.htm

[2] eds,W. Arden, M. Brillouët, P. Cogez, M. Graef, B. Huizing, R. Mahnkopf, "More-than-Moore, White Paper", ITRS publication, (2010)

[3] T. Kobayashi, H. Abe, Y. Niimura, T. Yamada, A. Kurosaki, T. Hosen, and T. Fujihira, "High voltage power MOSFETs reached almost to the silicon limit", Proc. ISPSD, pp.435 -438 2001

[4] G. Deboy, N. Marz, J. -P. Stengl, H. Strack, J. Tihanyi, and H. Weber, "A new generation of high voltage MOSFETs breaks the limit line of silicon", IEDM Tech. Dig., pp.683 -685 1998

[5] D. Kendig, K. Yazawa, and A. Shakouri, "Thermal Imaging of Encapsulated LEDs", Proceedings of the 27th IEEE SEMI-THERM Symposium, (2011), pp 310-313.

[6] K. Yazawa, D. Kendig, D. Hernandez, K. Maize, S. Alavi, A. Shakouri, High Speed Transient Thermal imaging of Microelectronic Devices and Circuits, EDFA Magazine Volume 15, No 1. (2013), pp. 12-22

[7] T. Skotnicki, J.A. Hutchby, T.-J. King H.-S.P. Wong, F. Boeuf, "The end of CMOS scaling: toward the introduction of new materials and structural changes to improve MOSFET performance", Circuits and Devices Magazine, IEEE, Vol. 1, Issue 1, (2005), pp. 16-26.

[8] C. M. Creveling, *Tolerance Design: A Handbook for Developing Optimal Specifications*, Addison-Wesley, 1996

[9] S. Alavi, K. Yazawa, G. Alers, B. Vermeersch, J. Christofferson and A. Shakouri, Thermal Imaging for Reliability Characterization of Copper Via, Proceedings of 27th IEEE SEMI-THERM Symposium, (2011), pp 17-20.

[10] D. Kendig, G.B. Alers, A. Shakouri, Thermoreflectance Imaging of Defects in Thin-Film Solar Cells, Proceedings IEEE International Physics Reliability Symposium IRPS2010, (2010), pp.499-502.

[11] B. Vermeersch, J. Christofferson, K. Maize, A. Shakouri, G. De Mey. Time and frequency domain CCD-based thermoreflectance techniques for high-resolution transient thermal imaging, Proceedings of IEEE 26th SEMI-THERM, (2010), pp. 228-234.

[12] G. Tessier, M. L. Polignano, S. Pavageau, Thermoreflectance temperature imaging of integrated circuits: calibration technique and quantitative comparison with integrated sensors and simulations, Journal of Physics D: Applied Physics 39, (2006), pp. 4159–4166

[13] E Matatagui, AG Thompson, M Cardona, Thermoreflectance in semiconductors, Physical Review, (1968).

[14] K. Yazawa, D. Kendig, P. E. Raad, P. L. Komarov, A. Shakouri, Understanding the Thermoreflectance Coefficient for High Resolution

Copyright © 2013 by ASME

Thermal Imaging of Microelectronic Devices, Technical Brief, Electronics Cooling Magazine, Issue March 2013, (2013), pp. 10-14.
[15] J. Christofferson, K. Yazawa, A. Shakouri, “Picosecond Transient Thermal Imaging Using a CCD Based Thermoreflectance System”, Proceedings of the 14th International Heat Transfer Conference, IHTC, (2010).
[16] K. Yazawa, D. Kendig, J. Christofferson, A. Marconnet, and A. Shakouri, Ultrafast Transient and Steady State Thermal Imaging of CMOS Integrated Circuit Chips with and without Package Thermal Boundaries, Proceedings of ITherm 2012 - Inter Society Conference on Thermal Phenomena, (2012).
[17] M. A. Green, “Self-consistent optical parameters of intrinsic silicon at 300 K including temperature coefficients”, Solar Energy Materials and Solar Cells, Vol. 92, Issue 11, (2008), pp 1305–1310.
[18] D.S.H. Chan, S.L. Tan, W.B. Len, K.H. Yim, L.S. Koh, C.M. Chua, L.J. Balk, A review of near infrared photon emission microscopy and spectroscopy, Proceedings of the 12th International Symposium on the Physical and Failure Analysis of Integrated Circuits, IPFA 2005, (2005), pp. 275 - 281

Copyright © 2013 by ASME